Available online at www.sciencedirect.com
ScienceDirect
Journal of the European Ceramic Society 29 (2009) 2491–2497
www.elsevier.com/locate/jeurceramsoc

Capillary rise properties of porous mullite ceramics prepared by an extrusion method using organic fibers as the pore former

Kiyoshi Okada[a,b,*], Shuhei Uchiyama[a], Toshihiro Isobe[a], Yoshikazu Kameshima[a], Akira Nakajima[a], Taisuke Kurata[c]

[a] *Department of Metallurgy and Ceramics Science, Tokyo Institute of Technology, 2-12-1 O-okayama, Meguro, Tokyo 152-8552, Japan*
[b] *Materials and Structures Laboratory, Tokyo Institute of Technology, 4259 Nagatsuta, Midori, Yokohama, Kanagawa 226-8503, Japan*
[c] *Kurata Refractory Co. Ltd., Hirono, Futaba, Fukushima 979-0402, Japan*

Received 12 December 2008; received in revised form 10 March 2009; accepted 16 March 2009
Available online 14 April 2009

Abstract

Porous mullite ceramics with unidirectionally oriented pores were prepared by an extrusion method to investigate their capillary rise properties. Rayon fibers 16.5 μm in diameter and 800 μm long were used as the pore formers by kneading with alumina powder, kaolin clay, China earthen clay and binder with varying Fe_2O_3 contents of 0, 5 and 7 mass%. The resulting pastes were extruded into cylindrical tubes (outer diameter (OD) 30–50 mm and inner diameter (ID) 20–30 mm), dried at room temperature and fired at 1500 °C for 4 h. The bulk densities of the resulting porous ceramics ranged from 1.31 to 1.67 g/cm^3, with apparent porosities of 43.2–59.3%. The pore size distributions measured by Hg porosimetry showed a sharp peak at 10.0 μm in the sample without Fe_2O_3 and at 15.6 μm in the samples containing Fe_2O_3; these pores, which arose from the burnt-out rayon fibers, corresponded to total pore volumes ranging from 0.24 to 0.34 ml/g. SEM showed a microstructure consisting of unidirectionally oriented pores in a porous mullite matrix. Prismatic mullite crystals were well developed on the surfaces of the pore walls owing to the liquid phase formed by the Fe_2O_3 component added to color the samples. The bending strengths of the tubular samples ranged from 15.6 to 26.3 MPa. The height of capillary rise, measured under controlled relative humidities (RH) of 50, 65 and 85%, was greater in the ceramics containing Fe_2O_3 than in those without Fe_2O_3, especially in the thinner samples. The maximum capillary rise reached about 1300 mm, much higher than previously reported. This excellent capillary rise ability is thought to be due to the controlled pore size, pore distribution and pore orientation in these porous mullite ceramics.

Keywords: Capillary rise; Extrusion; Porosity; Mullite; Functional applications

1. Introduction

Porous ceramics are widely used in various applications and require a variety of properties such as porosity, pore size, pore size distribution and volume, surface chemical properties, etc., depending on the application. To satisfy such a variety of requirements, various preparation methods[1] have been developed, such as partial sintering,[2] foaming,[3] etc. The most common preparation method for porous ceramics is the partial sintering of a ceramic powder using organic matter as a pore former, but it is difficult to produce products having both high permeability and good mechanical strength, because of the poor control of the porous microstructure resulting from this method. By contrast, we have developed porous ceramics with highly unidirectionally oriented through-hole pores by an extrusion method using flammable fibers as the pore formers.[4–8] In this preparation method, the fibers dispersed in the ceramic matrix tend to orient unidirectionally because of the flow of the ceramic paste during extrusion, producing through-hole pores with unidirectional orientation after the flammable fibers are burnt out. In this paper we describe the ceramics with this characteristic microstructure as "lotus ceramics". These lotus ceramics have high gas permeability (5×10^{-13} to 5×10^{-14} m^2)[7] and good mechanical bending strength (171 MPa)[4] at about 40% porosity, based on the controlled porous microstructure.

* Corresponding author at: Department of Metallurgy and Ceramics Science, Tokyo Institute of Technology, 2-12-1 O-okayama, Meguro, Tokyo 152-8552, Japan. Tel.: +81 3 5734 2524; fax: +81 3 5734 3355.
E-mail address: okada.k.ab@m.titech.ac.jp (K. Okada).

0955-2219/$ – see front matter © 2009 Elsevier Ltd. All rights reserved.
doi:10.1016/j.jeurceramsoc.2009.03.012

Table 1
Chemical compositions, shrinkages, bulk densities, apparent porosity and bending strengths of the samples.

Sample	Chemical composition			Fiber content [mass%]	Shrinkage [%]		Bulk density [g/cm^3]	Apparent porosity [%]	Bending strength [MPa]
	SiO2	Al2O3	Fe2O3		Drying	Firing			
Fe0	30	70	0	17.5	4.3–4.8	0.4–0.5	1.43–1.44	59.3	15.6
Fe5	36	56	5	20	5.3–5.4	2.1	1.57	46.6	22.8, 23.2
Fe7	38	51	7	20	6.0–6.7	1.4–2.7	1.62–1.66	43.2–44.4	23.7, 26.3

The porous microstructure occurring in these lotus ceramics resembles the microstructures of the xylem of plants, which are well known to efficiently pump water from the roots to the leaves, from which vapor evaporates. Since this is one of the cooling mechanisms of trees, we investigated the capillary rise and cooling effect of lotus ceramics.[9] Comparison of the capillary rise ability with that of other ceramics reported to show this property indicates that lotus ceramics have a superior capillary rise ability and higher capillary rise height than reported in other ceramics.[10,11] The observed surface temperature difference of lotus ceramics in the wet and dry state was nearly 10 °C when the dry sample was heated by sunlight to about 40 °C. Thus, ceramics with good capillary rise height ability are very efficient in reducing the effect of solar heating up to a height at which their surface is wetted. Since we previously had lotus ceramics only 400 mm in length, the capillary rise height of this lotus material could not be measured because the water appeared at the top of the samples within 1 h. The capillary rise height (h) is related to the pore radius (r) by the following Eq. (1):

$$h = \frac{2\gamma \cos\theta}{\rho g r} \tag{1}$$

where γ is the surface tension of water, θ is the contact angle between water and the pore wall, ρ is the density of water and g is gravitational acceleration. The relationship between the capillary rise height and pore radius is written as $h = 1.49 \times 10^{-5}/r$, assuming a contact angle (θ) = 0°, γ = 73 mN/m, $\rho = 1 \times 10^3$ kg/m^3 and g = 9.8 m/s^2. Thus, the capillary rise height increases with decreasing pore size of the lotus ceramics. However, it is also necessary to take into account the rate of capillary rise because smaller pore sizes are expected to markedly decrease this rate. The rate of capillary rise height is given by the Washburn eqation[12]:

$$h^2 = \frac{r_{\text{eff}}\gamma \cos\theta\, t}{2\eta} \tag{2}$$

where r_{eff} is the effective pore radius, t is the time and η is the viscosity of water. From this equation it is apparent that rate of capillary rise becomes greater with larger pore sizes. Thus, there is a trade-off between the pore size and the capillary rise height and rate. The value of r_{eff} equals r when all the pores are the same size (the ideal state). Thus, the capillary rise height is written as $h = (36.5 r_{\text{eff}} t)^{0.5}$, assuming γ = 73 mN/m and η = 1.00 Pa s. However, if there is a pore size distribution in the sample, as is generally the case, r_{eff} is not the same as the average pore radius and becomes smaller, markedly decreasing the rate of capillary rise. For these general cases, Patro et al.[11] proposed the following approximate calculation method for r_{eff}:

$$r_{\text{eff}} = \frac{r_{\text{min}}^4}{r_{\text{max}}^3} \tag{3}$$

where r_{min} and r_{max} are the minimum and maximum pore radii of the pores involved in the capillary rise. Using these equations, we have extrapolated the capillary rise height of the lotus ceramics[9] as a function of time and estimated a capillary rise height greater than 1000 mm.

In the present study, lotus ceramics 800–1800 mm in length were prepared by an extrusion method using rayon fibers as the pore formers and their capillary rise ability was determined.

2. Experimental procedure

The starting powders were alumina (Showa Denko, Japan), kaolin clay from Kentucky, USA (Morimura, Japan) and Chinese earthen clay (Inagaki Mining, Japan). The average particle sizes of these powders were 4.7, 1.0 and 20 μm, respectively. The Chinese clay was used to color the samples yellow-brown. Three bulk compositions listed in Table 1 were formulated with Fe_2O_3 contents of 0, 5 and 7 mass%. The powder batches were dry mixed with 20 mass% rayon fibers (Hope RB3.3Dtex Tow, Omikenshi, Japan) of average fiber diameter 16.5 μm and chopped to 800 μm lengths by Chubu Pile Ind., Japan. The mixtures were kneaded with 40 mass% water and molded using an extruder (Setogawa Industries, Japan). The dimensions of the extruder barrel and inner aperture were 95 and 30 (or 50) mm, respectively. Tubular green bodies with inner and outer diameters of 20–30, 30–50 and 20–50 mm were extruded using an outlet die. Thinner tubes of 20 and 30 mm ID and OD, respectively, were used for mechanical measurements. The extruded green bodies were dried at room temperature for 3 days, then at 120 °C for 18 h before being fired at 1500 °C for 4 h in air. Samples were designated Fen(m), where n and m represent the Fe_2O_3 content and thickness of the samples.

The bulk density and porosity of the samples was measured by the Archimedes technique using water. The pore size distribution and pore volume of the samples was measured by mercury intrusion porosimetry (Pascal 240, Carlo Elba, Italy) with a maximum injection pressure of about 200 MPa. The contact angle and surface tension used for the calculation was 130° and 0.485 N/m, respectively. The four-point bending strengths were measured using unpolished tubular samples Ø30 mm–Ø20 mm × 180 mm in size. The microstructure of the cut surface was observed using a scanning electron microscope (JSM-5310, JEOL Japan). The crystalline phases in the samples were examined by pow-

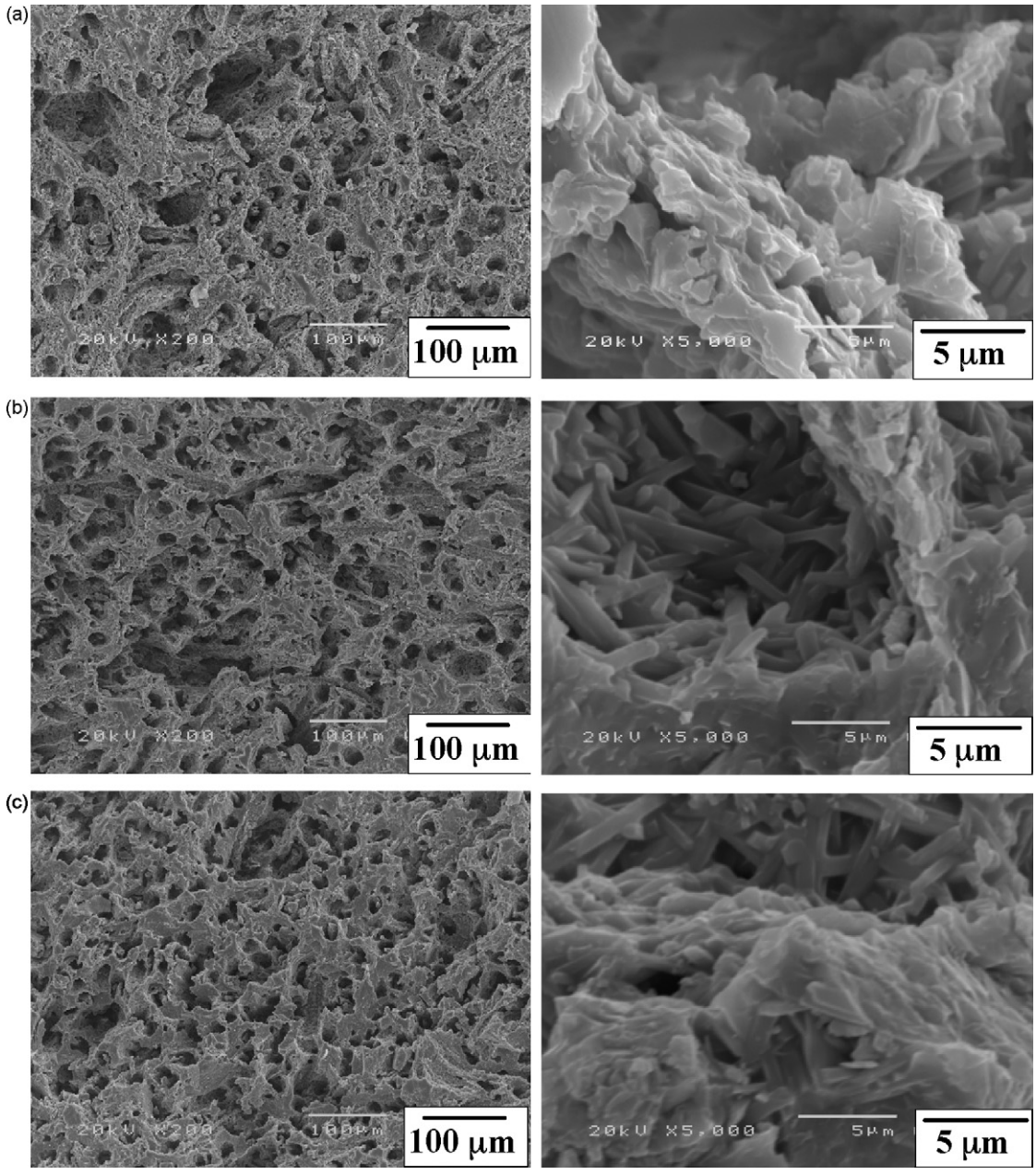

Fig. 1. SEM micrographs of cross-sections of the samples perpendicular to the extrusion direction. (a) Sample Fe0(5), (b) sample Fe5(5) and (c) sample Fe7(5).

der X-ray diffraction (XRD; XRD-6100, Shimadzu, Japan) with monochromated Cu Kα radiation.

The capillary rise ability of the samples (Ø40 mm–Ø20 mm × 1350 mm, Ø30 mm–Ø20 mm × 1350 mm and Ø50 mm–Ø20 mm × 1800 mm) were measured by immersing the one side (15 mm) in water at room temperature. The capillary rise height was measured at various time intervals by visual observation. The measurements were performed by controlling the RH to 50% (48–50%), 65% (56–69%) and 85% (78–90%) and the temperature to (21.5–24 °C). The measurement on the long sample (1800 mm in length) was performed under ambient conditions, the room temperature and RH during the measurements ranging between 15–22.5 °C and 32–61%, respectively.

3. Results and discussion

3.1. Characterization of the samples

Three different lotus ceramics with Fe_2O_3 contents of 0, 5 and 7 mass% were prepared, having different colors for potential applications as passive cooling wall materials. The drying shrinkages of the green bodies and firing shrinkages of the corresponding lotus ceramics are listed in Table 1. The drying shrinkages range from 4.3 to 6.7% and show a tendency to increase with increasing Fe_2O_3 content. The firing shrinkages of 0.4–2.7% are smaller than the drying shrinkage. A similar trend in the firing shrinkage was observed with the Fe_2O_3 content. The bulk densities of the samples (Table 1) range from

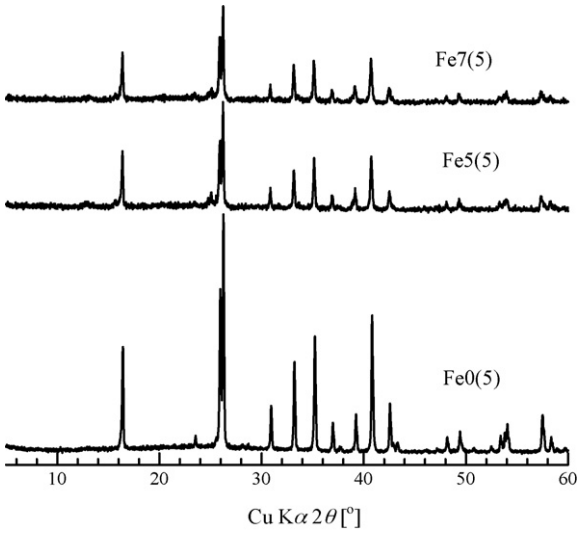

Fig. 2. XRD patterns of samples Fe0(5), Fe5(5) and Fe7(5).

1.31 to 1.66 g/cm^3 and the apparent porosities range from 43.2 to 57.3%. As expected from the shrinkage data, these values also show a clear trend with Fe_2O_3 content.

The bending strengths of the three samples (Table 1) increase from 15.6 MPa in sample Fe0(5) to 23.0 MPa in sample Fe5(5), to 26.3 MPa in sample Fe7(5). This trend is also consistent with the measured shrinkage, bulk density and apparent porosity of the samples.

The SEM micrographs of cross sections of three samples perpendicular to the extrusion direction are shown in Fig. 1(a)–(c), respectively. All the samples show similar porous structures with dispersed pores corresponding to the cross sections of the cylindrical pores formed by burn-out of the rayon fibers. The pore sizes (about 15–20 μm diameter) agree well with those of the original rayon fibers. The degree of orientation of the cylindrical pores in these samples is not as high as reported in samples using carbon fibers as the pore formers.[4] The reasons for this are related to differences in the size of the starting powders, the amount and type of lubricant, extrusion conditions and size of the extruded samples. The microstructure of the matrix in sample Fe0(5) (Fig. 1(a)) differs from samples Fe5(5) (Fig. 1(b)) and Fe7(5) (Fig. 1(c)). The microstructure of the sample Fe0(5) consists of irregularly shaped mullite grains with a relatively porous matrix texture. Formation of mullite was confirmed from the XRD pattern (Fig. 2). This microstructure is attributed to incomplete sintering due to the starting powders being too coarse for mullite sintering at this firing temperature.[13] The weak bending strength of this sample (Table 1) is due to this partial sintering in the absence of a liquid phase formed by the coloring agent at high temperature. By contrast, the microstructures of the matrix of samples Fe5(5) and Fe7(5) consist of elongated mullite grains (Fig. 2) with an interlocking aggregated microstructure. The development of the mullite grains is especially significant on the surfaces of the pores formed by the burn-out of the rayon fibers. Such a microstructure is thought to be formed by liquid phase sintering due to the small amount of Fe_2O_3 added to color the samples.[13] The addition of Chinese clay as the coloring agent therefore not only changes the color of the sample from white to yellow-brown but also densifies the matrix by liquid phase formation at high temperatures. Enhancement of the densification of these samples produces increased mechanical bending strengths >20 MPa.

The pore size distributions (PSDs) of three samples measured by Hg porosimetry are shown in Fig. 3. As expected from the differences in the microstructures of the samples with and without Fe_2O_3, the PSDs are also different. The PSD of sample Fe0(5) shows a steep increase in the cumulative pore volume at about 12 μm, corresponding to a sharp peak in the relative pore volume curve at 10 μm. Since the full width at half maximum (FWHM) of this pore size peak is 2 μm, the minimum pore radius (r_{min}) and maximum pore radius (r_{max}) is estimated to be 4 and 6 μm, making r_{eff} = 1.19 μm (from Eq. (3)). These pores are considered to correspond to the burnt-out rayon fibers. The cumulative pore volume curve shows a second increase at about 1 μm, corresponding to the pores in the mullite matrix. By contrast, the cumulative pore volume curves of samples Fe5(5) and Fe7(5) both show steep increases at pore sizes of about 20 μm, giving a sharp peak in the relative pore volume curve at 15.6 μm. The FWHM values of these peaks (about 2.3 μm) are slightly larger than for sample Fe0(5). The r_{min} and r_{max} values of both sample Fe5(5) and Fe7(5) are estimated to be 6.7 and 9.0 μm respectively, corresponding to a value of r_{eff} calculated from Eq. (3) to be 2.80 μm; this value is larger than that of sample Fe0(5). The cumulative pore volume curves of these samples do not show a second increase as in sample Fe0(5), indicating a densified matrix. The total pore volumes of the three samples follow the order sample Fe7(5) (0.24 ml/g) <sample Fe5(5) (0.28 ml/g) <sample Fe0(5) (0.34 ml/g). The sizes of pores formed by burnt-out of the rayon fibers are different in sample Fe0(5) from those in samples Fe5(5) and Fe7(5). This is because the pore sizes are not directly related to the diameter of fibers used. As already reported,[7] the through-hole pores of lotus ceramics are formed by contact between a number of fibers. Therefore, the resulting pore sizes measured by Hg porosimetry correspond to the pores formed by fiber contact, called pore contact ($P_{contact}$). This $P_{contact}$ depends on the sizes of the fibers and the ceramic particles, and also on the packing of the ceramic particles in the paste. In the present case, the $P_{contact}$ values of samples Fe5(5) and Fe7(5) are larger because of the densification of these samples by liquid phase sintering.

3.2. Capillary rise ability

The samples used for the capillary rise ability test were tubular samples with thin walls (5 mm) and thick walls (10 mm) and were all 1350 mm long. The capillary rise heights of three samples are shown in Fig. 4(a)–(c) as a function of time. The observed capillary rise height increased steeply initially, but this increase gradually declined with time. The capillary rise heights differed between the samples and at different RH conditions. These differences were larger at low RH due to the greater influence of water vapor evaporation from the surface. The capillary rise ability of the samples was therefore compared using the data at RH = 85% which were less affected by water vapor evapora-

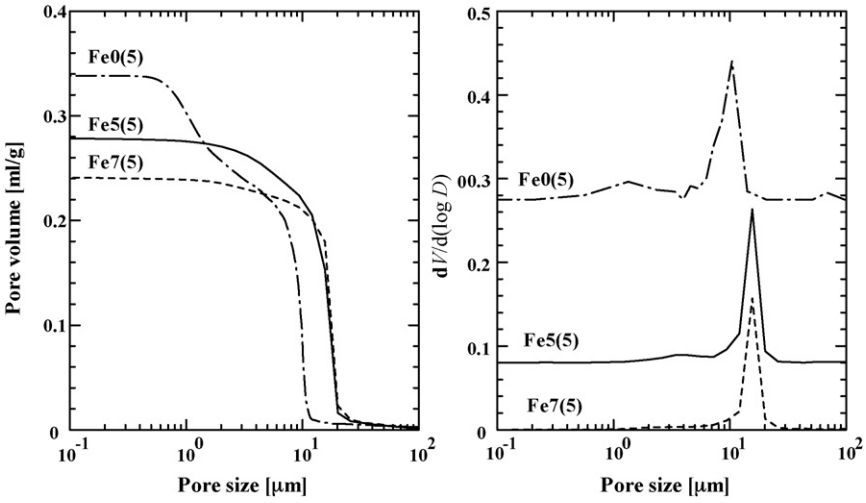

Fig. 3. Pore size distributions of samples Fe0(5), Fe5(5) and Fe7(5) measured by Hg porosimetry.

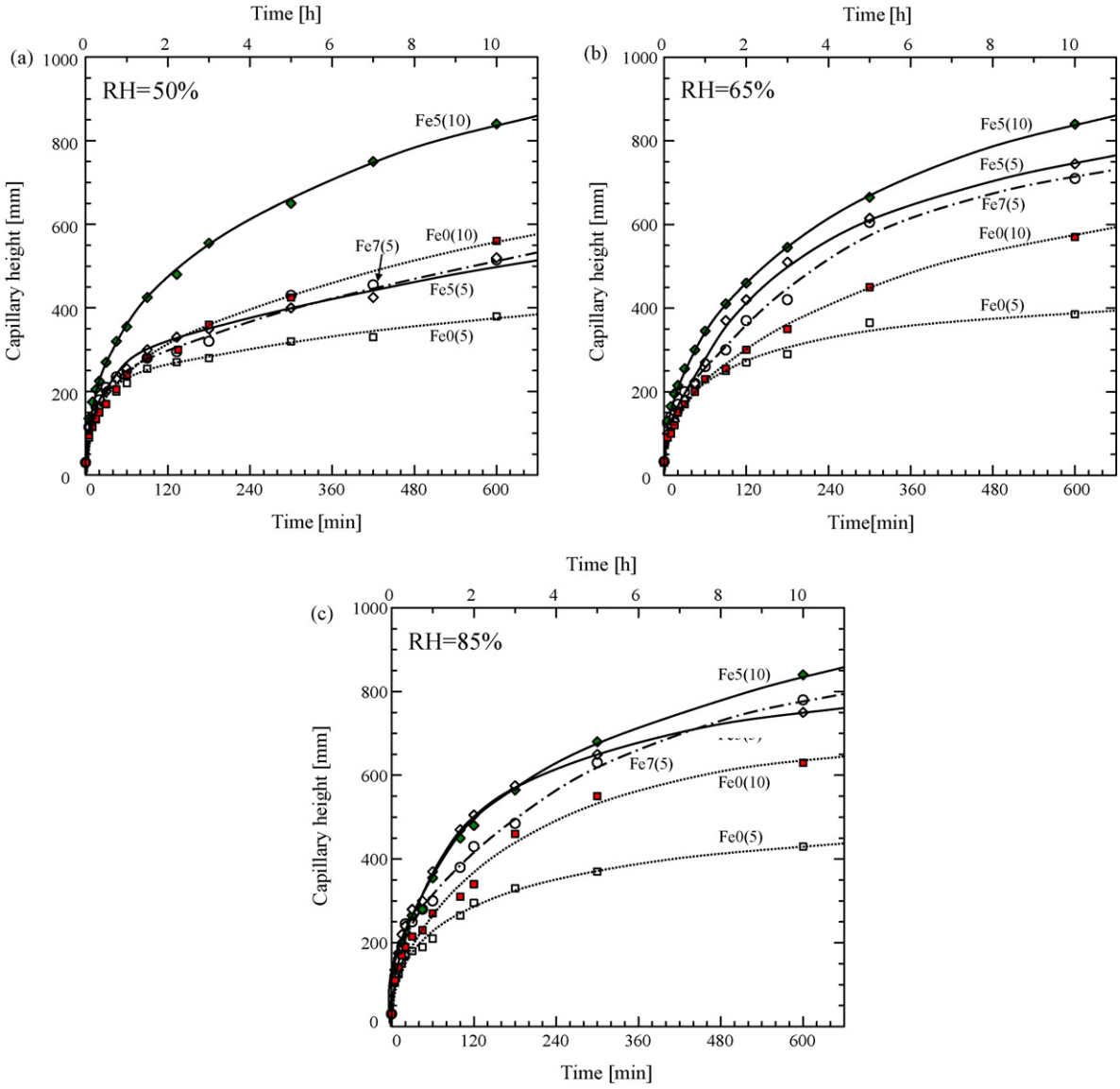

Fig. 4. Changes of capillary rise heights as a function of time for various samples. (a) RH = 50%, (b) RH = 65% and (c) RH = 85%.

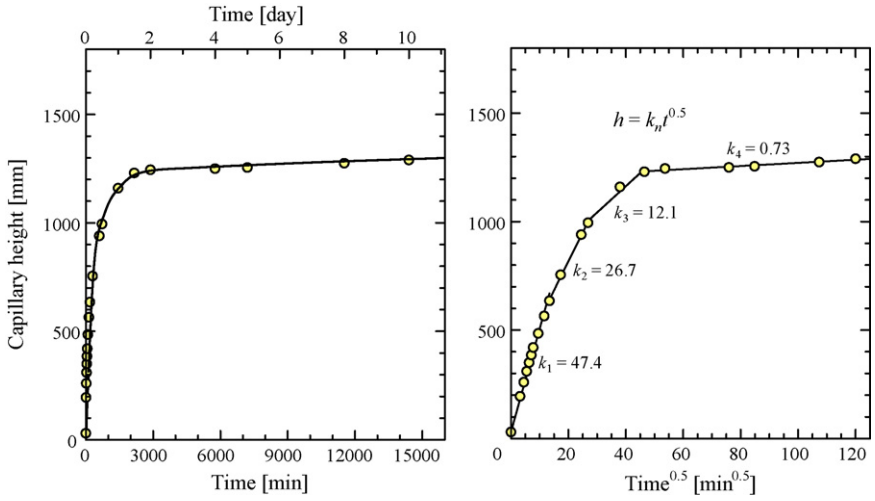

Fig. 5. Observed capillary rise height of sample Fe5(15) as a function of time and time$^{0.5}$.

tion. There was a clear difference in the behavior of samples with and without Fe_2O_3, the former showing the greater capillary rise ability. We suggest three main reasons for this difference, i.e. the Fe_2O_3-free sample has (1) a smaller pore radius (r) and effective pore radius (r_{eff}), (2) a lower number of capillary pores due to the lower mixing ratio of rayon fibers, and (3) a porous matrix. There was also a difference in the capillary rise ability corresponding to the thickness of tubes; the thicker tubes (10 mm) showed a higher ability than the thinner tubes (5 mm). This may be due to the lower volume/surface ratio of the thin-walled samples. Although the capillary rise curves of samples Fe0(5) and Fe0(10) differed according to the RH conditions, this was not true of sample Fe5(10), i.e. there was no influence of surface evaporation in this sample.

The capillary rise curve of the long sample Fe5(15) is shown in Fig. 5. This lotus ceramic is found to have a capillary rise height of up to 1300 mm, the highest of all samples so far reported. The experimental data show a linear relationship in the h vs. $t^{0.5}$ plot that can be divided into four different stages of the experiment, suggesting four different time stages.

If the resulting maximum capillary rise height of 1300 mm is assumed to be the equilibrium height (h_{eq}) of this sample, the contact angle (θ) of this sample is calculated from Eq. (1) to be 47°. This calculated value is reasonable because contact angles of various silicate ceramics are generally 30–50°.[14] In order to enhance the capillary height of lotus ceramics, higher wettability and/or smaller pore radius may be needed.

Models have been proposed for capillary rise phenomena by previous workers.[15–17] Zhmud et al.[15] pointed out inconsistencies in the classical equations and proposed a simplified general relation for the capillary rise dynamics corresponding to the long-time limit based on a diffusion-controlled process, giving the following Eq. (4):

$$h_Z = \left(\frac{2\gamma\cos\theta}{\rho g r}\right)\left(1 - \exp\left(\frac{-\rho^2 g^2 r^3 t}{16\eta\gamma\cos\theta}\right)\right) \quad (4)$$

On the other hand, Fries and Dreyer[16,17] proposed analytical solutions for four defined time stages as follows:

(1) purely inertial time stage:

$$h_1 = \left(\frac{2\gamma\cos\theta}{\rho r}\right)^{0.5} t \quad (5)$$

(2) visco-inertial time stage:

$$h_2 = \left(\frac{\gamma r\cos\theta}{2\eta}\right)^{0.5}\left(t - \left(1 - \exp\left(\frac{-8\eta t}{r^2\rho}\right)\right)\right)^{0.5} \quad (6)$$

(3) purely viscous time stage:

$$h_3 = \left(\frac{\gamma r\cos\theta}{2\eta}\right)^{0.5} t^{0.5} \quad (7)$$

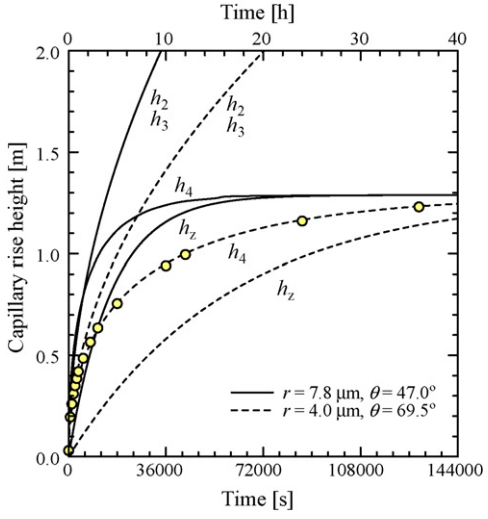

Fig. 6. Calculated and observed capillary rise height as a function of time. The solid and broken lines h_2, h_3, h_4 and h_Z are calculated using $\theta = 47°$ and $r = 7.8$ μm while the broken lines are calculated using $\theta = 69.5°$ and $r = 4.0$ μm.

(4) viscous and gravitational time stage:

$$t = -\left(\frac{8\eta}{\rho g r^2}\right) h_4 - \left(\frac{16\eta\gamma\cos\theta}{\rho^2 g^2 r^3}\right) \times \ln\left(1 - \left(\frac{\rho g r}{2\gamma\cos\theta}\right) h_4\right) \quad (8)$$

The capillary rise curves predicted by Eqs. (4) and (6)–(8) were calculated using the parameters $\gamma = 72\,\text{mN/m}$, $\theta = 47^\circ$, $\rho = 997\,\text{kg/m}^3$, $g = 9.8\,\text{m/s}^2$, $r = 7.8\,\mu\text{m}$ and $\eta = 9.11 \times 10^{-4}\,\text{kg/m s}$. These are shown in Fig. 6, together with the experimental data for sample Fe5(15). None of the calculated curves of h_z, h_2, h_3 and h_4 (solid lines) fit the observed data well when using the parameters of $r = 7.8\,\mu\text{m}$ (from Hg porosimetry data) and $\theta = 47^\circ$ (from h_{eq}). However, the curve h_4 calculated using $r = 4.0\,\mu\text{m}$ and $\theta = 69.5^\circ$ ($h_{eq} = 1.3$) showed an excellent fitting with the observed data. Although this pore size is very much different from that obtained from Hg porosimetry, this works like as the throat of the pore structure of the lotus ceramics and dominates the capillary rise rate and ability. We didn't expect such a high contact angle for the lotus ceramics but probably very rough surface of the microstructure of the pores as shown in Fig. 1 caused such a high contact angle. This suggests that capillary rise height higher than 1.3 m can be obtained by lowering of the contact angle by producing smoother pore surfaces.

4. Conclusion

Porous mullite ceramics were prepared by an extrusion method using rayon fibers as the pore formers, and their capillary rise ability was investigated, with the following results:

(1) An Fe_2O_3 component added for the purpose of coloring the samples significantly influences the microstructures of the porous mullite ceramics. Increasing Fe_2O_3 content increases drying and firing shrinkage, bulk density and mechanical strength, but decreases the apparent porosity and pore volume. The resulting pore size was about 10 μm in sample Fe0(5) (without Fe_2O_3) but was 15.6 μm in samples Fe5(5) and Fe7(5) (containing Fe_2O_3).
(2) A maximum capillary rise ability of 1300 mm was confirmed in sample Fe5(15), this value being the highest of those so far reported. The change of capillary rise height with time could be very well simulated using the equation (8) with the fitting parameters of $r = 4.0\,\mu\text{m}$ and contact angle (θ) = 69.5°. Since the resulting pore size is different from that obtained from Hg porosimetery ($r = 7.8\,\mu\text{m}$), it is considered to behave like the throat of the pore structure and dominate the capillary rise rate and height.

Acknowledgements

A part of this work was supported by the Grant for Application of Industrial Technology Innovation of the New Energy and Industrial Technology Development Organization of Japan (NEDO) under Contract No. 0827001. The authors thank Professors M. Daimon and E. Sakai of the Tokyo Institute of Technology for permitting the use of the instruments of Hg porosimetry. We also thank Professor K.J.D. MacKenzie of Victoria University of Wellington for critical reading and editing of this manuscript.

References

1. Saggio-Woyansky, J., Scott, C. E. and Minnear, W. P., Processing of porous ceramics. *Am. Ceram. Soc. Bill.*, 1992, **71**, 1674–1682.
2. Lam, D. C. C., Lange, F. F. and Evans, D. G., Mechanical properties of partially dense alumina produced from powder compacts. *J. Am. Ceram. Soc.*, 1994, **77**, 2113–2117.
3. Peng, H. X., Fan, Z., Evans, J. R. G. and Busfield, J. J. C., Microstructure of ceramics foams. *J. Eur. Ceram. Soc.*, 2000, **20**, 807–813.
4. Isobe, T., Tomita, T., Kameshima, Y., Nakajima, A. and Okada, K., Preparation and properties of porous alumina ceramics with oriented cylindrical pores produced by an extrusion method. *J. Eur. Ceram. Soc.*, 2006, **26**, 957–960.
5. Isobe, T., Kameshima, Y., Nakajima, A., Okada, K. and Hotta, Y., Extrusion method using nylon 66 fibers for the preparation of porous alumina ceramics with oriented pores. *J. Eur. Ceram. Soc.*, 2006, **26**, 2213–2217.
6. Isobe, T., Kameshima, Y., Nakajima, A., Okada, K. and Hotta, Y., Effect of dispersant on paste rheology in preparation of porous alumina with oriented pores by extrusion method. *J. Porous Mater.*, 2006, **13**, 269–273.
7. Isobe, T., Kameshima, Y., Nakajima, A., Okada, K. and Hotta, Y., Gas permeability of the porous alumina ceramics with uni-directionally aligned pores by extrusion method. *J. Eur. Ceram. Soc.*, 2007, **27**, 53–59.
8. Isobe, T., Kameshima, Y., Nakajima, A. and Okada, K., Preparation and properties of porous alumina ceramics with uni-directionally oriented pores by extrusion method using a plastic substance as a pore former. *J. Eur. Ceram. Soc.*, 2007, **27**, 61–66.
9. Okada, K., Kameshima, Y., Nakajima, A. and Madhusoodana, C. D., Preparation of lotus-type porous ceramics with high pump-up ability and its cooling effect by water vapor evaporation. *J. Heat Island Inst. Intern.*, 2007, **2**, 1–5.
10. Kubota, T., Sugimoto, H. and Komiya, H., Development of multifunctional green wall system using ceramic boards with pump-up ability. *Report Obayashi Tech. Inst.*, 2003, **67**, 1–6.
11. Patro, D., Bhattacharyya, S. and Jayaram, V., Flow kinetics in porous ceramics: understanding with non-uniform capillary models. *J. Am. Ceram. Soc.*, 2007, **90**, 3040–3046.
12. Washburn, E. W., The dynamics of capillary flow. *Phys. Rev.*, 1921, **17**, 273–283.
13. Schneider, H., Okada, K. and Pask, J. P., *Mullite and Mullite Ceramics*. John Wiley, London, 1994.
14. Maatta, J., Piispanen, M., Kuisma, R., Kymalainen, H. R., Uusi-Rauva, A., Hurme, K. R. *et al.*, Effect of coating on cleanability of glazed surfaces. *J. Eur. Ceram. Soc.*, 2007, **27**, 4555–4560.
15. Zhmud, B. V., Tiberg, F. and Hallstensson, K., Dynamics of capillary rise. *J. Colloid Interface Sci.*, 2000, **228**, 263–269.
16. Fries, N. and Dreyer, M., An analytic solution of capillary rise restrained by gravity. *J. Colloid Interface Sci.*, 2008, **320**, 259–263.
17. Fries, N. and Dreyer, M., The transition from inertial to viscous flow in capillary rise. *J. Colloid Interface Sci.*, 2008, **327**, 125–128.